**Network for Research and Development in Africa**
International Journal of Pure and Applied Science Research
ISSN: 2384-5918. Volume 12, Number 6
Pages 72-93 (August, 2023)
DOI: 67321673211269
https://arcnjournals.org

# 3D Seismic Attributes Analysis for Reservoir Characterization of Jaff Field offshore Niger Delta, Nigeria

**[1]Asoegwu, I. K., [2]Onuba, L. N., [3]Onyebueke, E. O., [4]Oparaku, O. I.**
[1, 3]Department of Industrial Physics, Chukwuemeka Odumegwu Ojukwu University, Uli Campus
[2]Department of Geology Chukwuemeka Odumegwu Ojukwu University, Uli Campus
[4]Department of Physics/Electronics, Federal Polytechnic Nekede, Imo State
Corresponding Authors Email: asoegwuiyke11@gmail.com

***Abstract:*** *Seismic attributes analysis for reservoir characterization was carried out across Jaff Field, offshore Niger Delta Basin, with the aim to identify possible hydrocarbon prospects away from currently producing zone within the field. Suite of wire-line logs and seismic volume was employed to gain more insight into the complexities of the hydrocarbon hosting units within the field. Mapping and interpretation of faults and horizons were carried out across the seismic volume. Well correlation (North-South direction), aided by gamma ray log were carried out across the field. Three reservoirs of interest (B-sand, C- Sand and D-Sand reservoirs), were delineated and correlated. Well to seismic tie revealed that the identified reservoir tops correspond nearly to the crests of seismic section. Time structural maps generated from these tops were subsequently converted to depth structural maps using available velocity model. From the maps, it was observed that the principal structure responsible for hydrocarbon entrapment in the field for the three identified reservoirs with their prospects are made up of a set of NW-SE trending normal faults. These faults correspond to the crest of roll over anticline. The prospects were further characterized by the presence of clusters of bright strong seismic attributes, (RMS, average envelop and average instantaneous frequency), showing the presence of hydrocarbon. Results from the study revealed that, away from currently producing zone at the central part of the field, additional lead and prospects exist within the field.*

***Keywords:*** *seismic, amplitudes, fault, hydrocarbon, structures, reservoirs.*

## INTRODUCTION

Structural interpretation serves as an important aspect of the development program of an oil field. It has diverse application in many areas of 3D seismic interpretation among which include: identifying and delineating structural and stratigraphic features associated with hydrocarbon generation, deposition, migration, and entrapment, which are the main goal of hydrocarbon exploration (Telford *et al.,* 1990). These structural and stratigraphic traps could be very subtle and are, therefore, difficult to map accurately. Subsurface configurations must be understood in detail to effectively delineate the structures that are favorable for hydrocarbon accumulation (Coffen, 1984). This is because hydrocarbons are found in geologic

traps, (rock structure that will keep oil and gas from escaping either vertically or laterally). These traps can either be structural or stratigraphic.
On the other hand, seismic attributes analysis has come a long way since their introduction in the early 1970s and they have become an integral part of seismic interpretation. Various methodologies have been developed for their application to broader hydrocarbon exploration and reservoir characterization. According to Doust, *et al.,* (1990) majority of the traps in the Niger Delta are structural. Therefore, the focus in this study was channeled towards mapping the structural traps available within the study area and delineating hydrocarbon prospect using seismic attributes as direct hydrocarbon indicators (DHIs).
Given the benefits of these seismic attributes, some key attributes were applied to enhance reservoir characterization in Jaff Field. They were used to resolve serious interpretational challenges associated with sub-seismic faults and subtle stratigraphic features which most often result to poor seismic resolution.

## GEOLOGY OF THE STUDY AREA

The "Jaff Field" lies within the Coastal Swamp Depobelt of the Niger Delta oil province. It is located within longitude 05˚41'27"E to 05˚42'05"E and latitude 05˚51'55"N to 05˚52'03"N on the western part of Niger Delta (Figure 1). The field contains six wells and all was selected specifically for the purpose of this study. The Niger Delta Basin covers an area of approximately 75,000 km$^2$ and consists of an overall regressive clastic sequence, whose maximum thickness is about 12 km in the central part, (Short and Stauble, 1967). It ranks among the world's most prolific petroleum producing tertiary deltas that together account for about 5% of the world oil reserve and for 2.5% of the present-day basin of the earth (Reijer *et al.,* 1997).

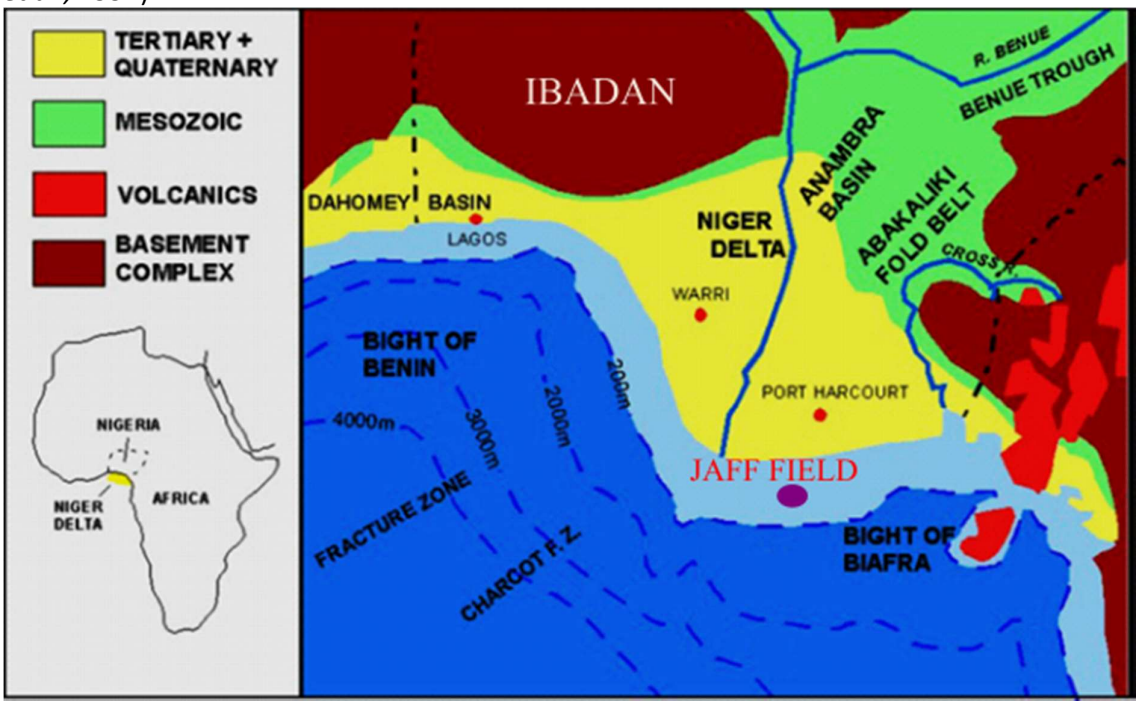


**Figure 1: Geological Map of Niger Delta Basin showing the study area (Modified from Ajisafe and Ako, 2013)**.

**LITHOSTRATIGRAPHY OF THE NIGER DELTA**

The sedimentary sequence as formed in the subsurface of the Niger Delta has been modified by numerous transgressions which occurred from time to time, breaking the continuity of the main overall regression and becoming stratigraphically superimposed. The tertiary section of the Niger Delta is divided into three broad formations (Figures 2) representing prograding depositional facies that are distinguished mostly on the basis of sandshale ratio. Stratigraphically, the Tertiary Niger Delta is divided into three formations, namely Akaka formation, Agbada formation, and Benin formation (Evamy *et al.,* 1978; Etu, 1997).

The Akaka formation at the base of the delta is predominantly undercompacted, overpressured sequence of thick marine shales (Potential Source Sock), clays and siltstone (Potential Reservoirs in deep water). Beginning in the Paleocene and through the Recent, the Akata Formation formed during low stands when terrestrial organic matter and clays were transported to deep water areas characterized by low energy conditions and oxygen deficiency (Michele *et al.,* 1999). The marine shale is typically over pressured. It is the deepest formation and it is made up of marine shale, clays and silts that underlie the deltaic sequence (Figure. 2). It is the source rock i.e., where hydrocarbon is generated before migrating to Agbada Formation.

The Agbada Formation which is the major petroleum bearing unit began in the Eocene and continues into the Recent. The formation consists of paralic clastic of over 3700 m thick and represents the actual deltaic portion of the sequence. Shale and sandstone beds were deposited in equal proportions; however, the upper is mostly sand with only minor shale interbeds (Figure 2). The sequence is associated with sedimentary growth faulting and contains the bulk of the hydrocarbon reservoirs.

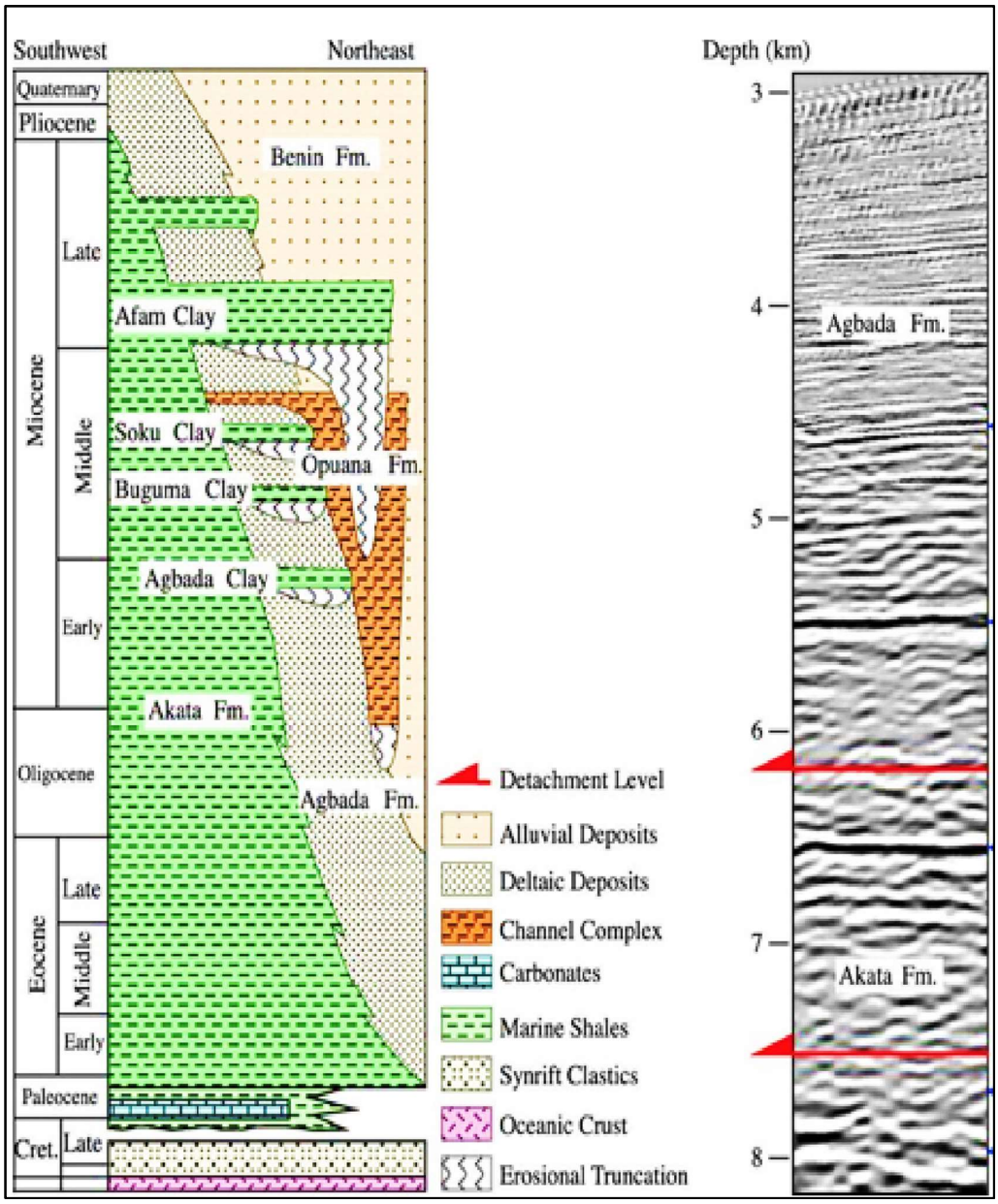


**Figure 2: Niger Delta Basin Synopsis of lithostratigraphic units. (Reijers *et al.,* 1997).**

The Benin formation is the shallowest part of the sequence and is composed almost entirely of non- marine sand (Figure 2). It is a continental latest Oligocene to Recent deposit of alluvial and upper coastal plain that are up to 2000 m thick (Tuttle *et al.,* 1999). It is deposited in the upper coastal plain environments following a southward shift of deltaic deposition into a new Depobelt. Benin formation is the youngest formation in the Niger Delta. The formation consists of massive, highly porous, freshwater bearing sandstones with local thin shale interbed which is considered to be of braided stream origin. The sand and sandstone of the Benin formation are coarse to fine grain in general and are poorly sorted (Tuttle *et al.,* 1999).

## METHODOLOGY

The 3D SEG-Y seismic reflection data available for this study include a base map and a 3D seismic volume. The data is a post-stack data, zero-phase, with central frequency of 22.81 Hz and dominant bandwidth of 65 Hz. The data processing, interpretation and analysis consist of three main steps that includes delineation of hydrocarbon-bearing sands from well-log correlation and analysis. The analysis of suites of composite logs was aimed at a qualitative and quantitative determination of the properties of delineated reservoirs. The gamma ray (GR) and spontaneous potential (SP) logs were examined for lithology information.
Secondly, carrying out well-to-seismic tie in order to establish a relationship between the seismic data and well log data. This helps to represent the interfaces and intervals interpreted on the seismic data set with those same markers and units in the well penetration with a high level of accuracy. Finally. mapping faults and horizons in order to understand the structural framework and trapping mechanisms in the field. In this case, fault picking and horizon mapping was achieved by adopting approaches to ensure consistency in interpretation. These were done to accurately determine the exact horizons as the top of a potential reservoirs. Seismic attribute maps (Root mean square (RMS) Amplitude, Instantaneous Frequency, and Average Envelope) was also generated to further indicate areas of bright spots which show hydrocarbon presence.

## RESULTS AND DISCUSSION

### Well Log Data Analysis

The resistivity log in combination with the GR log were used to differentiate between hydrocarbon and non-hydrocarbon bearing zones. Lithological correlation of equivalent strata across four wells (TMB-01, TMB-02, TMB-04, TMB-05,) was performed by matching for similarities the intervals of logs from different wells. At the same time, the potential hydrocarbon reservoirs (Sand B, Sand C and Sand D) in the various wells were delineated. The outcome of the identified potential hydrocarbon reservoirs correlation across the four wells were shown in figure 3-5.

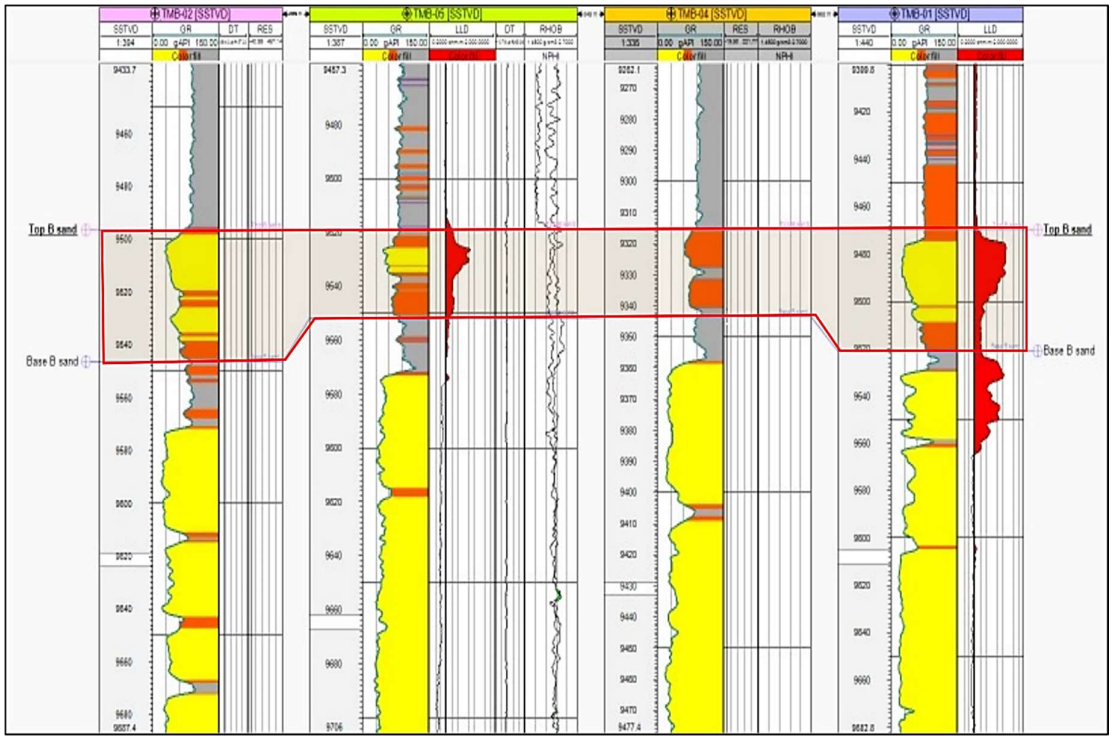


**Figure 3: Well Correlation of B-Sand across four (4) wells, showing the top and base of the Sand B reservoir.**

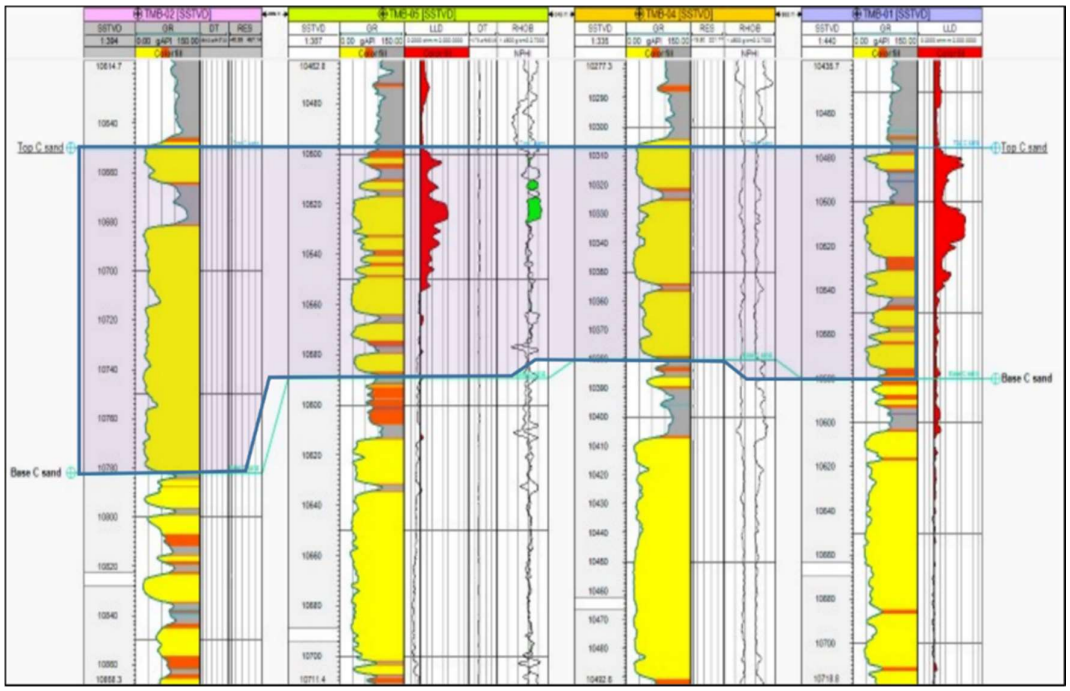


**Figure 4: Well Correlation of C-Sand across four (4) wells, showing the top and base of the reservoir.**

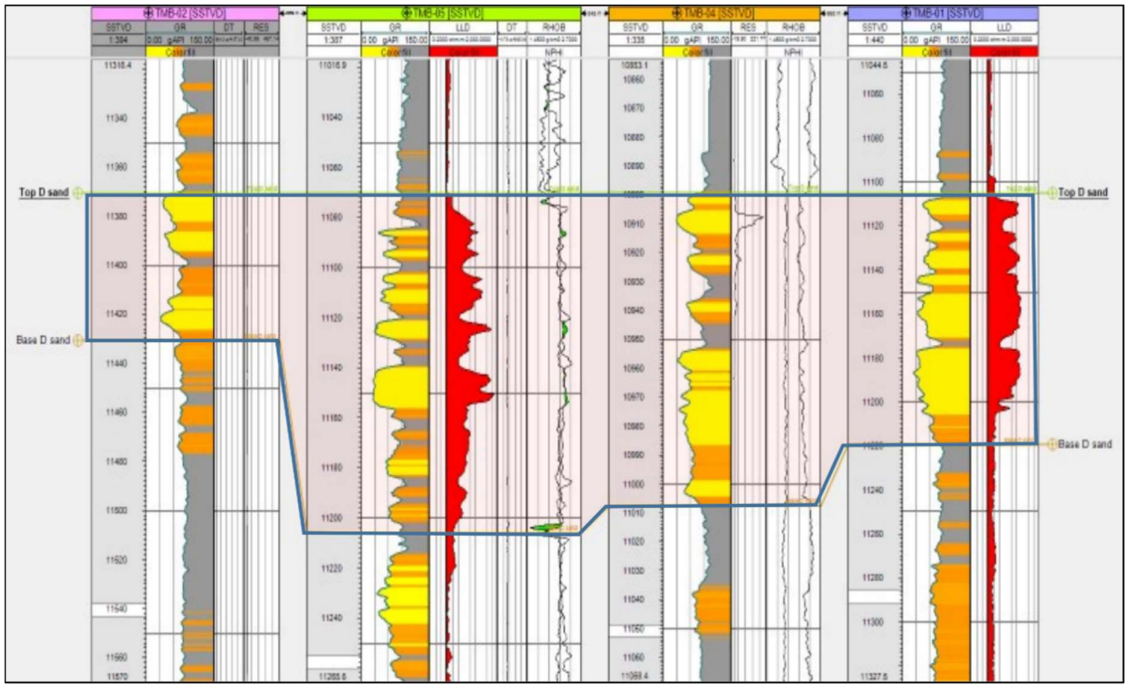


**Figure 5: Well Correlation of D-Sand across four (4) wells, showing the top and base of the Sand D reservoir.**

## Well -to- seismic ties

The tops of the mapped reservoirs on well logs were tied to seismic data using the available checkshot data of the well TMB-05. In this procedure, the product of the wireline logs; Sonic (DT) and Bulk Density (RHOB), which provide the inverse velocity and density information of subsurface gives the acoustic impedance (Z). Then the Z was used to compute a series of reflection coefficients called reflectivity series. This reflectivity series was later convolved with the Recker wavelet of frequency 22.81Hz for sonic calibration, and subsequent generation of the synthetic seismogram which were used for seismic-to-well tie (Figure 6).

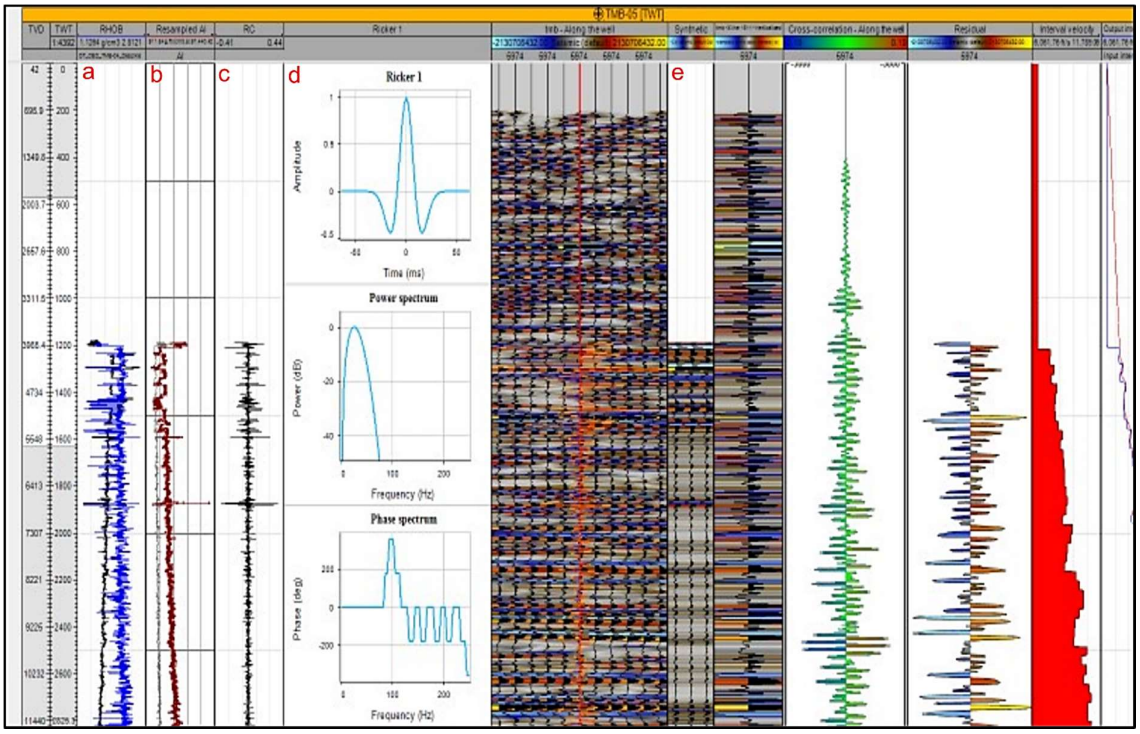


**Figure 6: Synthetic Seismogram generation. (a) Black is sonic log and blue is density log. (b) Resampled acoustic impedance (A.I.) (c) Reflectivity series. (d) Wavelet with amplitude and phase spectrum. (e) The product Seismogram.**

The synthetic seismogram was compared with the original seismic, but the crests and the troughs of both do not match. Then a bulk shift of 4ms at 2ms sample rate was generated, and was use to give a near-perfect match between the original seismic and synthetic seismogram (Figure 6). The crests (red amplitudes) are high impedance events, while the troughs (blue amplitudes) are low impedance events. The well-tie revealed that the identified reservoir tops correspond nearly to the crests of original seismic. A borehole model was generated and used to correlate the seismic crossline (1611) section together with the synthetic seismogram and the wireline log (Figure 7).

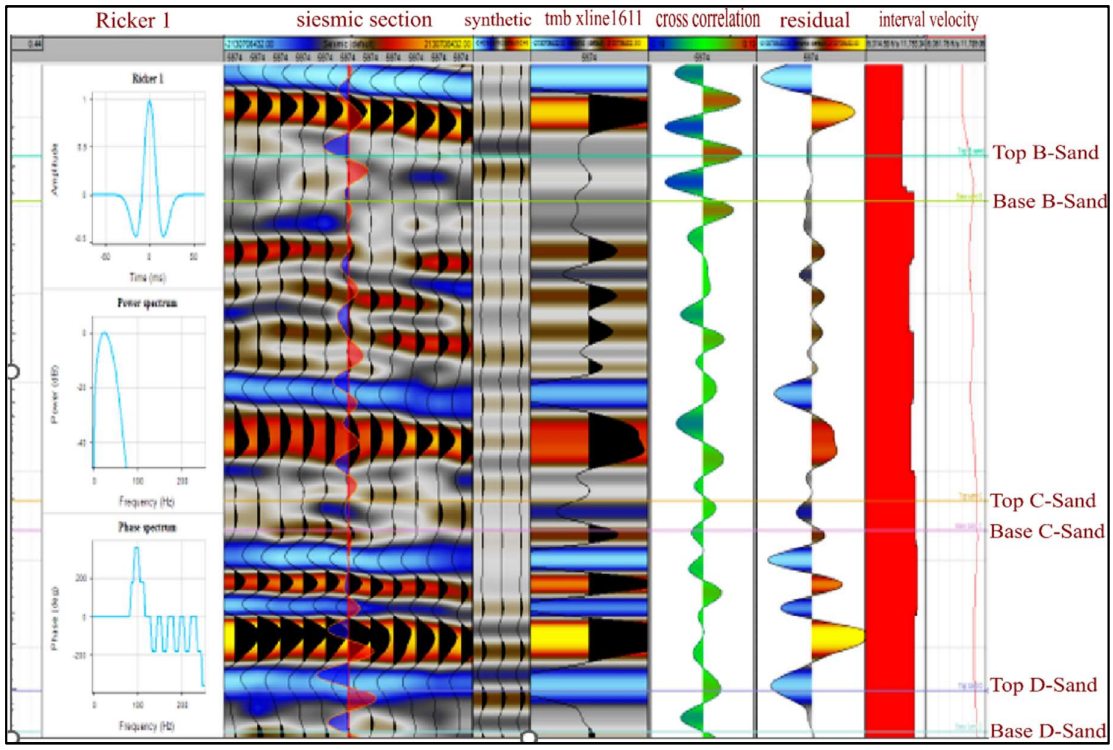


**Figure 6: Seismic-to-Well tie for well TMB-05 showing the top and base of the identified reservoirs of Jaff Field offshore Niger Delta.**

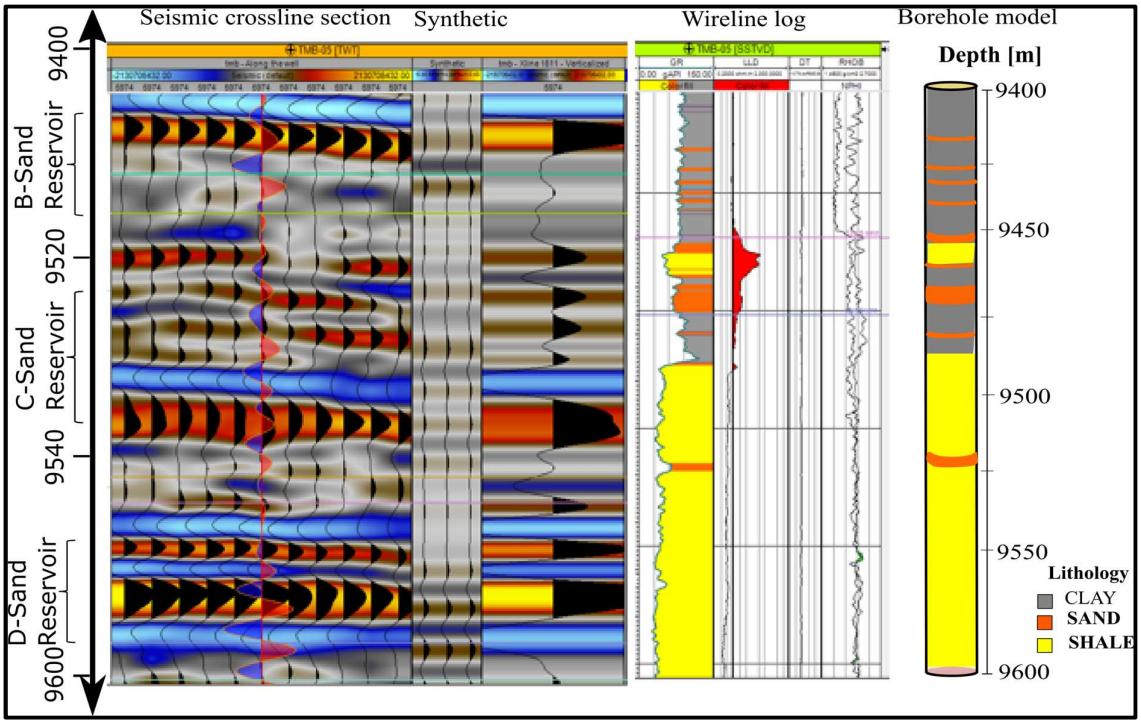


**Figure 7: Cross correlation of the borehole model, seismic crossline section with the synthetic seismogram and the wireline log.**

## Seismic interpretations

The interpretation was performed where dataset, geometry and seismic attribute volumes already exist. The 3D seismic
reflection data was imported into the interpretative tool by creating a 3D reflectivity volume (steering cube) of inline, cross line and time slide of the seismic data (Figure 8).

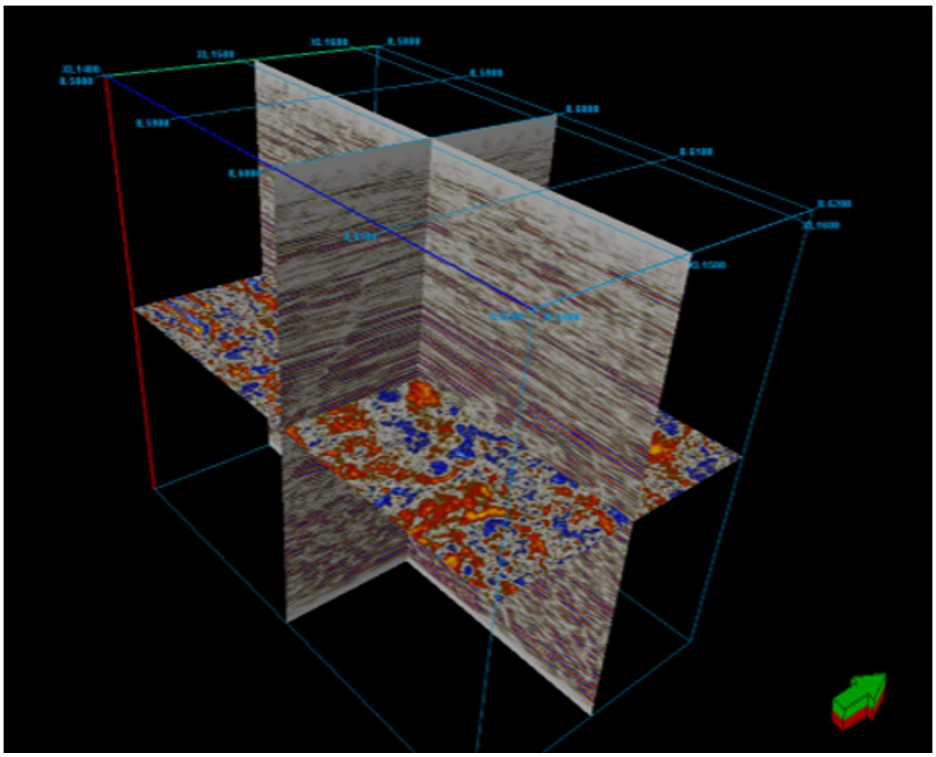

**Figure 8: The steering cube, showing the 3D view of inline, cross line and time slice of Jaff Field offshore Niger Delta**

## Fault interpretation

The structural geometry of the Jaff Field was carried out by picking assigned fault segments on the seismic sections. Figure 9a shows the vertical seismic section as well as the Structural Smoothening attributes (structural attributes) generated from the seismic volume around inline 6000 showing enhanced visualization of the fault system and the pronounced dip of the faults.
The seismic section displays several faults, which are visible as non-continuous reflections aligned in a specific direction, along with amplitude distortions around the fault zone and changes in the dip of events. A total of eight faults were identified, and were marked using various line colors (Figure 9b). Among these, four faults (F1, F2, F3, and F4) were selected from the inline section 6180 (Figure 9a). The faults labeled as F1, F2, and F3 are primarily regional growth faults, with F1 being the major growth fault within the field. These faults dip towards the South (Basinward) away from the direction of sediment supply. On the other hand, fault F4 is classified as an antithetic fault, dipping towards the Northeast.

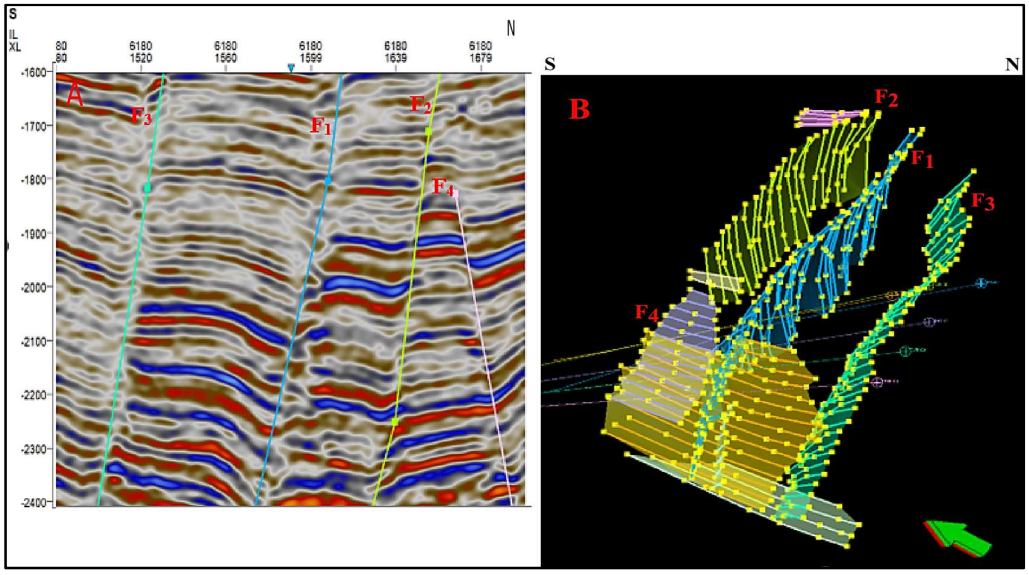


**Figure 9: (a) Interpreted faults sticks, extracted from 3D seismic section inline 6180. (b) 3D View of the interpreted faults of Jaff Field offshore Niger Delta.**

## Horizon interpretation

A horizon is an imaginary surface in the subsurface of the earth, usually thought of representing a stratigraphic surface (either lithostratigraphic or chronostratigraphic).

In this research work, three horizons ($H_1$, $H_2$ and $H_3$) corresponding to the three identified reservoirs tops (B-Sand, C-Sand and D-Sand) were construed and built on the connection to the well TMB-05 on the seismic cube. Well, TMB-05 was the only well with checkshot data (used for well-to-seismic-tie) and the three horizons fall on the trough (negative polarity) of the time slide. These three interpreted horizons were within the Agbada Formation, (table 1) with an appropriate control of the well tops for the three reservoirs. The selected formation tops were posted on the seismic section and correlated across the surface of the study area. The three horizons were mapped on both 2D and 3D seismic sections across the field in order to understand the vertical and horizontal variation of zones of interest. On the 3D seismic sections, the horizons were mapped on the inlines using a petrel time player interval of 10 units. The interpreted horizons, B-Sand, C-Sand and D-Sand on the inline 6090 were mapped at two-way time of 2550 ms, 2610 ms and 2770 ms respectively, towards the south. The horizons were also mapped in the middle block at time 2290 ms, 2360 ms and 2480 ms and in the north at time 2240 ms, 2280 ms and 2380 ms respectively as shown in figure 10. The horizons are greatly displaced by fault $F_1$ when compared to fault $F_2$. Fault $F_1$, gives a displacement throws of 260 ms to horizon B-sand, 250 ms to horizon C-sand and 290 ms to horizon D-Sand respectively. While fault $F_2$ gives a displacement throw of 50 ms, 80 ms and 100 ms for B-sand, C-Sand and D-Sand respectively on inline 6050 as shown in figure 10. The seismic horizons, B-sand, C-Sand and D-Sand are characterized by a medium to high amplitude with sub-parallel to parallel reflectors.

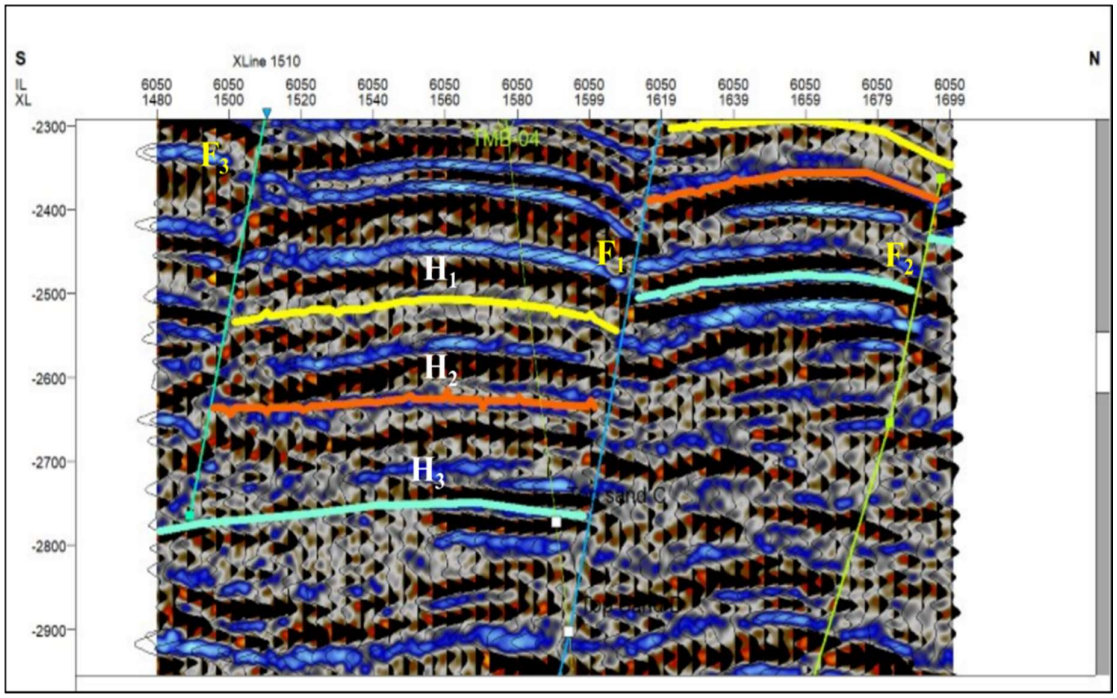


**Figure 10: Interpreted horizons from seismic section, inline 6050 of Jaff Field offshore Niger Delta.**

**Table 1: Information for the Analyzed Horizons**

| Horizons | Formation | Color |
|---|---|---|
| B-Sand | Agbada | |
| C-Sand | Agbada | |
| D-Sand | Agbada | |

## Velocity model

The velocity model was generated from checkshot data using the least square method of second-degree polynomial function (nonlinear velocity function) as shown in equation 1

$$Y = 28.1399 + 2.70106 \times X - 0.000472572 \times X^2 \quad 1$$

With a covariance of $1.7425E + 6$. This model converts the interpreted time subsurface horizons; B-Sand time surface, C-Sand time surface and D-Sand time surface to depth because subsurface structures such as faults and horizons interpreted in the seismic section are in time unit.

## Surface map generation and hydrocarbon prospects identification of Jaff Field

The surface time-structure elements in the field are made up of a set of NW-SE trending normal faults, describing a fault block in the northeastern part of the map. However, normal fault trending in the NE-SW was identified in the western region of the surface map. The lowest regions in the surface map are identified at the southern part of map while the highest elevation is found at the northeastern region of the surface map. The polynomial function (equation 1) was utilized to convert the time-structure surface maps to a depth-structure surface map.

## B-Surface structural maps

B-Surface time structural map displays a monocline structure ($F_1$, $F_2$, $F_3$ and $F_4$) dipping in the northern direction. The surface time map was generated by linking points of equal time. The time structure map of B-Surface was then converted to depth map using the polynomial nonlinear velocity function as shown in equation 1, generated from checkshot data of well TMB-05. The depth values within this surface range from - 8200 ft to -10800 ft.

From B-Surface depth map, five prospects were identified (prospects A, B, C, D and E) as shown in Figure 11. Prospect A has the largest zone (area) and forms a 3-way closure (fault dependent trap) while prospect E has the smallest zone (area). These five fault dependent traps were further characterized by the presence of clusters of bright strong seismic attributes, (RMS, average envelop and average instantaneous frequency), showing potentially the presence of hydrocarbon in the regions as indicated by the black dotted line as shown in Figure 12, 13 and 14. A lead was identified in the northeastern part of the B-surface and marked with the presence of strong seismic attributes.

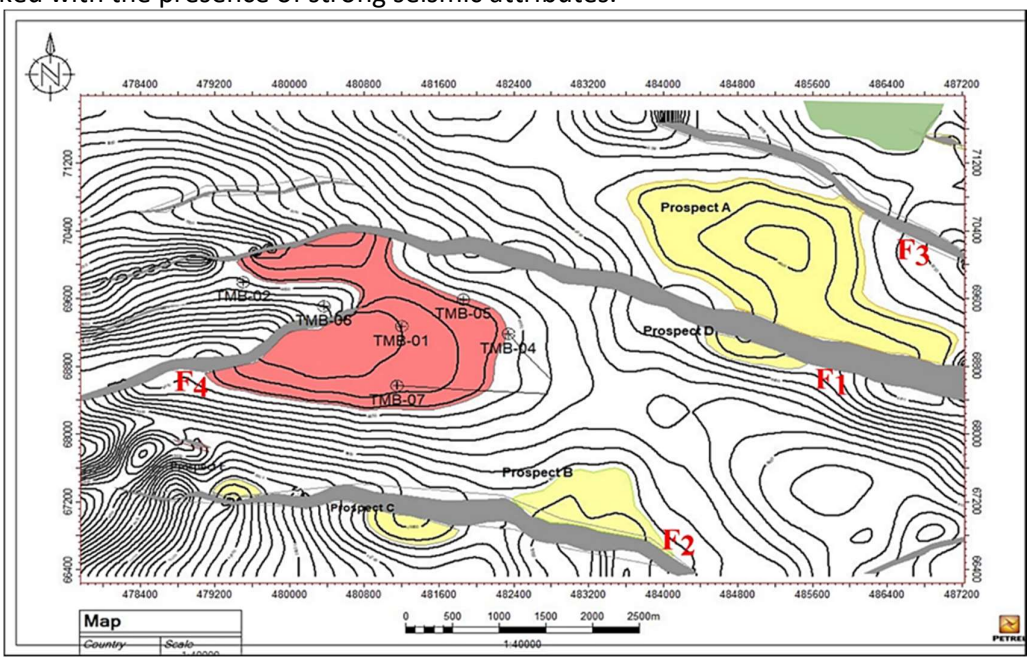


**Figure 11: Depth structural map for B-Surface showing identified prospects and lead of Jaff Field offshore Niger Delta**

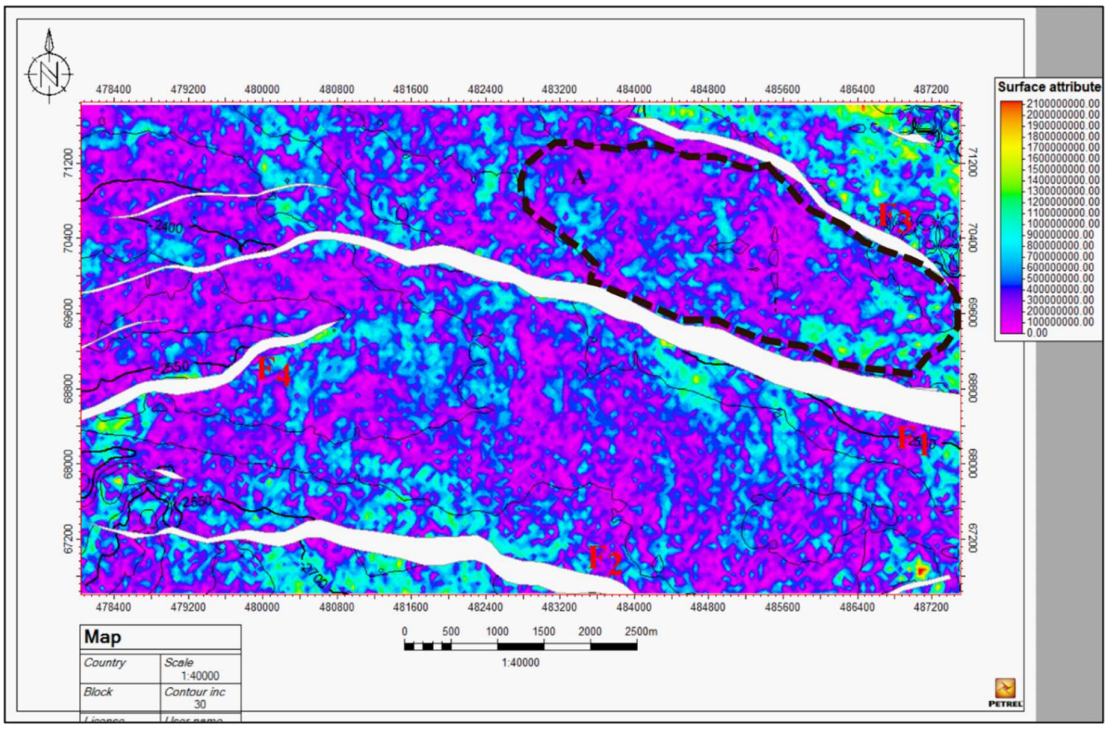


**Figure 12: RMS attribute map for B-Surface of Jaff Field offshore Niger Delta.**

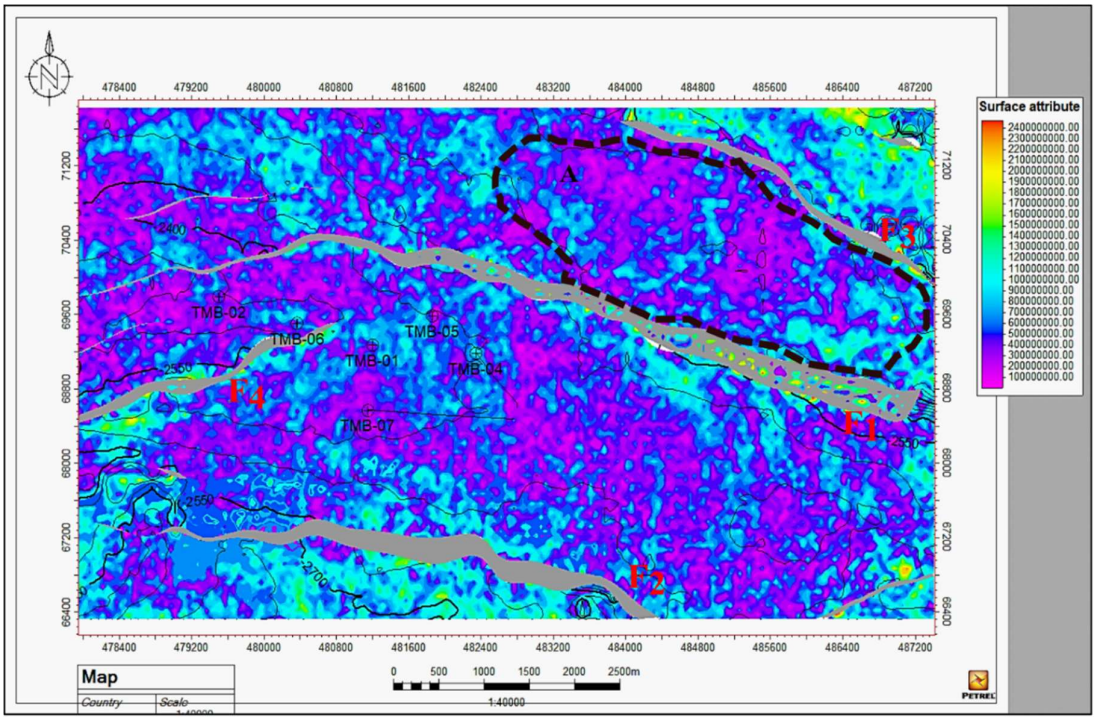


**Figure 13: Average Envelop attribute map for B-Surface of Jaff Field offshore Niger Delta.**

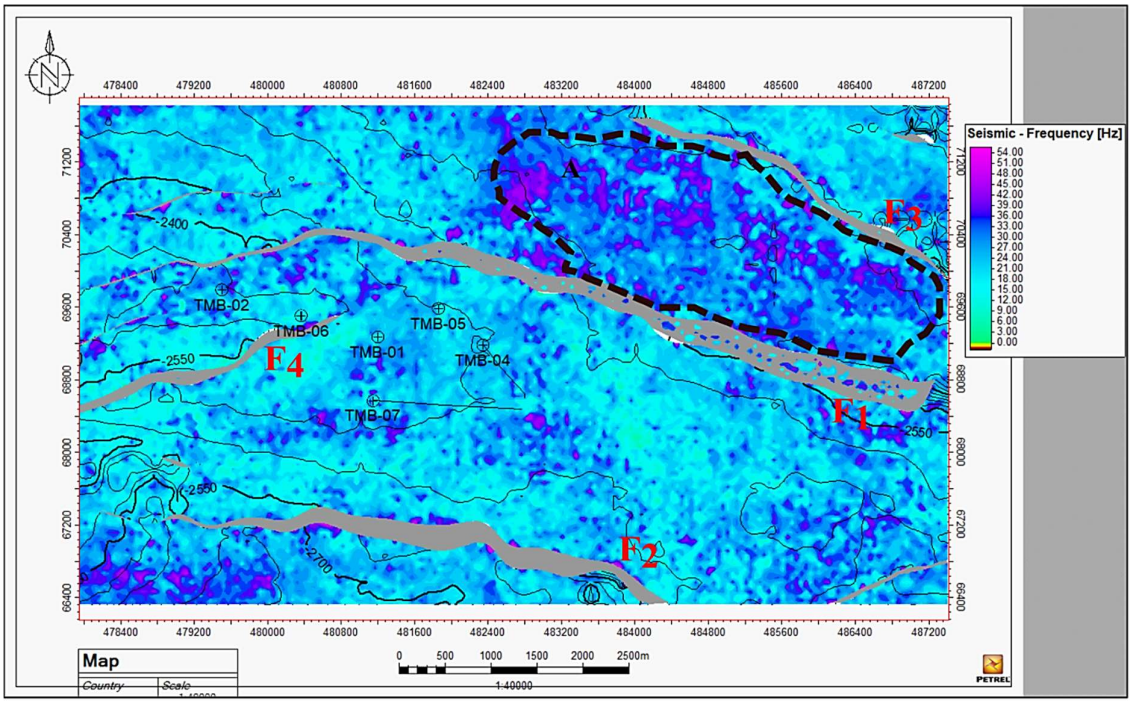


**Figure 14: Average Instantaneous Frequency attribute map for B-Surface of Jaff Field offshore Niger Delta.**

## C-Surface structural maps

C-Surface time structural map also displays a monocline structure ($F_1$, $F_2$, $F_3$ and $F_4$) dipping in the northern direction. The surface time map was generated by linking points of equal time. The time structure map of surface C was then converted to depth map using the polynomial nonlinear velocity function as shown in equation 4.1, generated from checkshot data of well TMB-05. The depth values within this surface range from -11200 ft to -6525 ft.

From C-surface depth map, only one prospect was identified in the northeastern part of the map, which is a fault dependent trap (3-way closure) as shown in Figure 15. This trap is characterized by the presence of clusters of strong root mean square (RMS), average envelop and average instantaneous frequency attributes indicating regions potentially saturated with hydrocarbon as indicated by the black dotted lines as shown in Figures 16, 17 and 18.

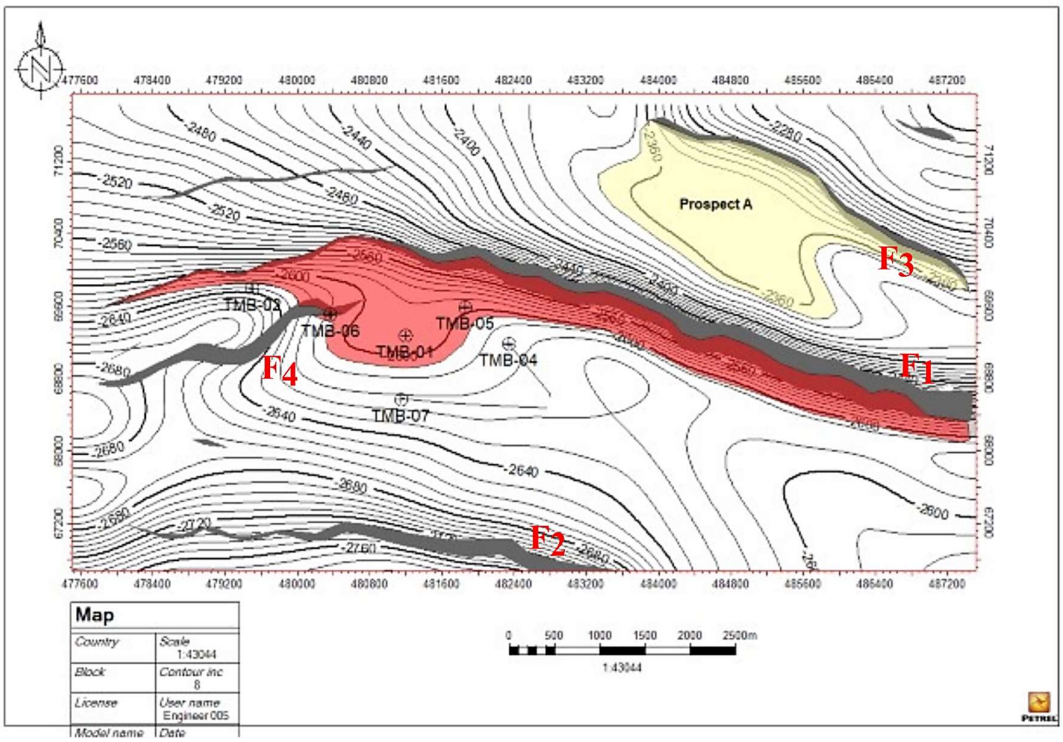


**Figure 15: Depth structural map for C-Surface showing identified prospect of Jaff Field offshore Niger Delta.**

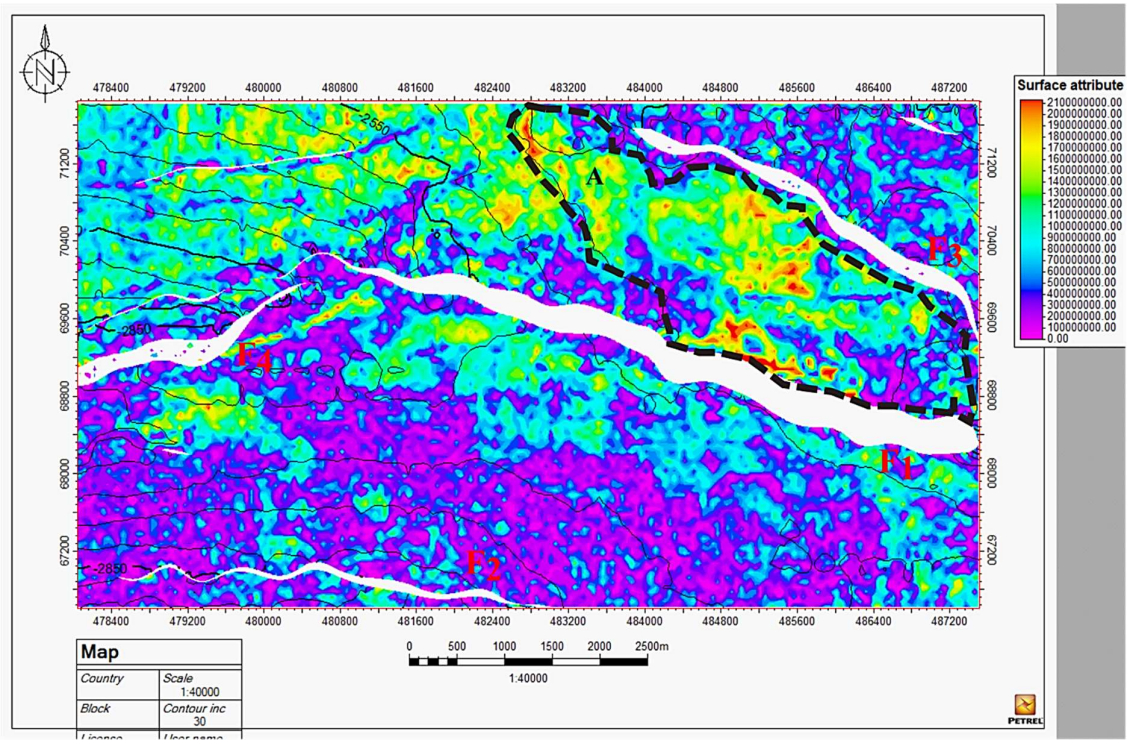


**Figure 16: RMS attribute map for C-Surface of Jaff Field offshore Niger Delta.**

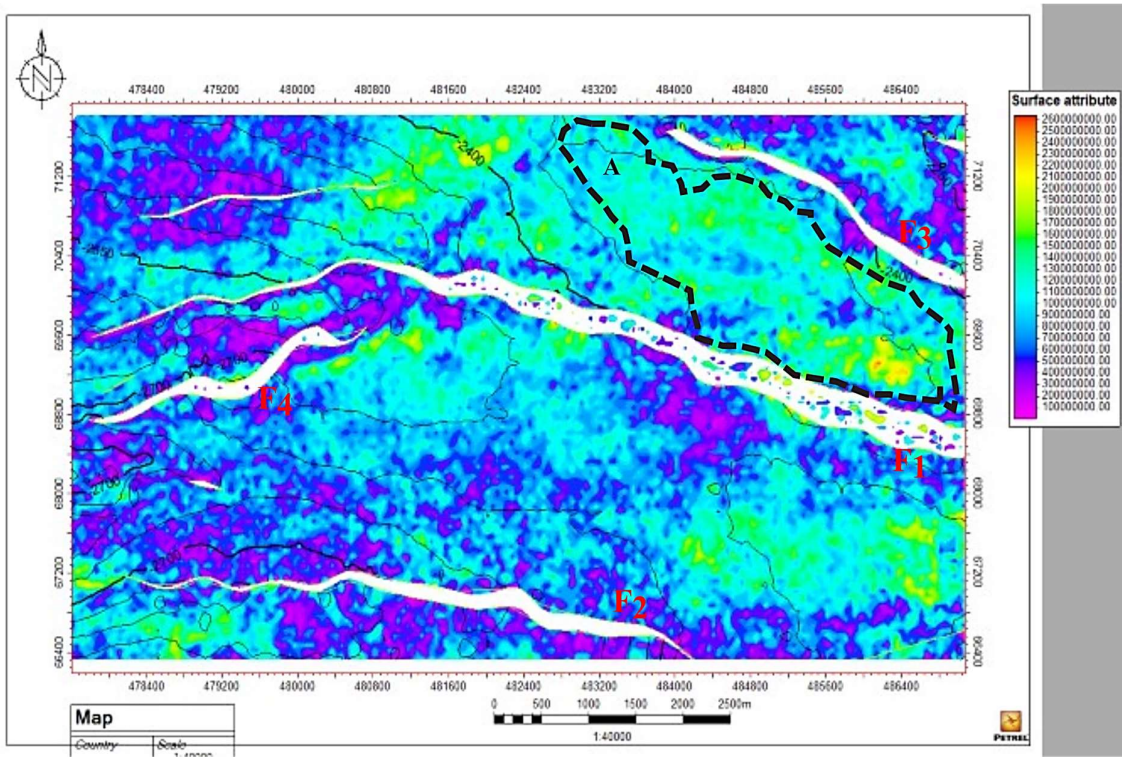


**Figure 17: Average Envelop attribute map for C-Surface of Jaff Field offshore Niger Delta.**

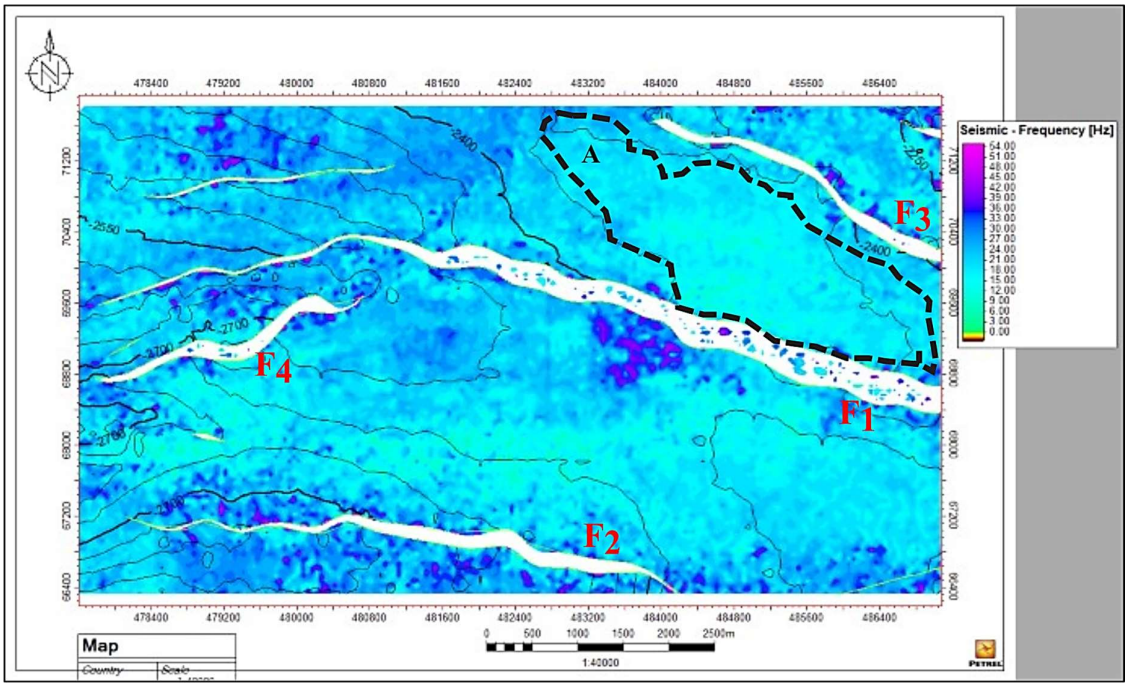


**Figure 18: Average Instantaneous Frequency attribute map for C-Surface of Jaff Field offshore Niger Delta.**

## D-Surface structural maps

Like B-Surface and C-Surface, D-Surface time structural map equally displays a monocline structure ($F_1$, $F_2$, $F_3$ and $F_4$) dipping in the northern direction. The surface time map was generated by linking points of equal time. The time structure map of surface D was then converted to depth map using the polynomial nonlinear velocity function as shown in equation 1, generated from checkshot data of well TMB-05. The depth values within this surface range from -2310 ft to -2940 ft.

Just as in C-Surface, single prospect was also identified in D-Surface depth map, which is located towards the northeastern part of the map (Figure 19). This prospect is bounded by two faults, forming a two-way structural trap. This region was characterized by the presence of strong RMS attribute. Average envelop and instantaneous frequency attribute were also generated and correlated with the RMS attribute. All these attributes show strong clusters of bright spots, indicating the presence of hydrocarbon indicated by the black dotted lines as shown Figures 20, 21 and 22. However, most of the wells in this region were discovery wells located in the western zone of the map (region marked with red color) as shown in Figure 19.

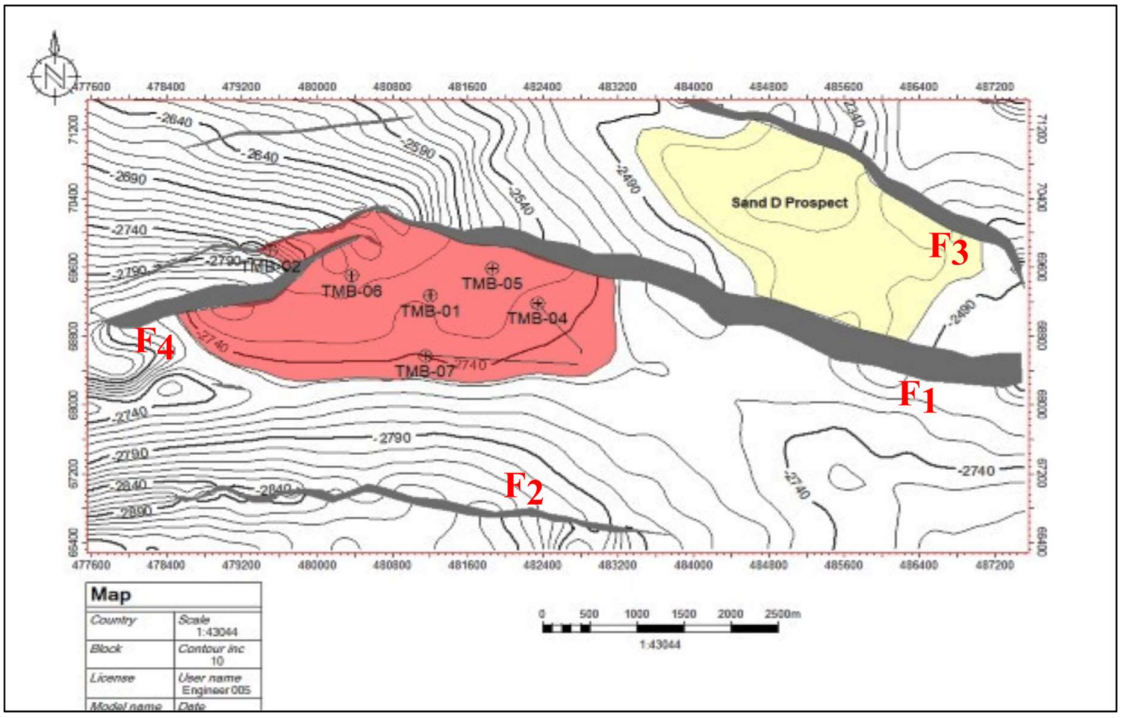


**Figure 19: Depth structural map for D-Surface showing identified prospect of Jaff Field offshore Niger Delta.**

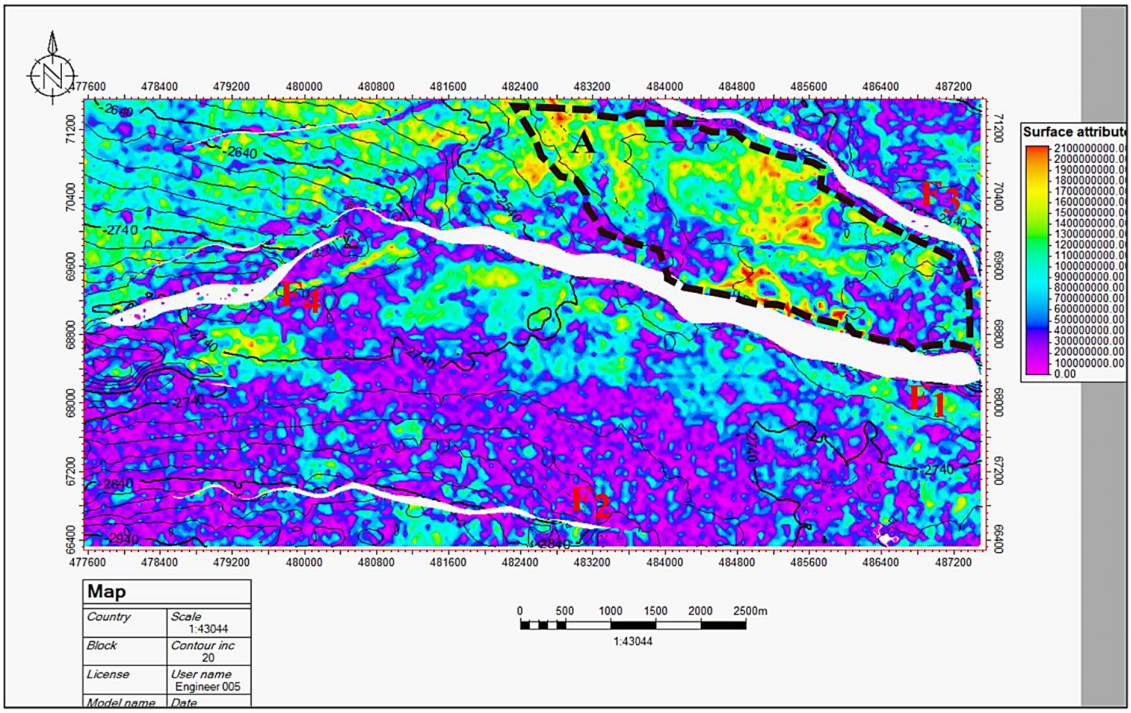


**Figure 20: RMS attribute map for D-Surface of Jaff Field offshore Niger Delta.**

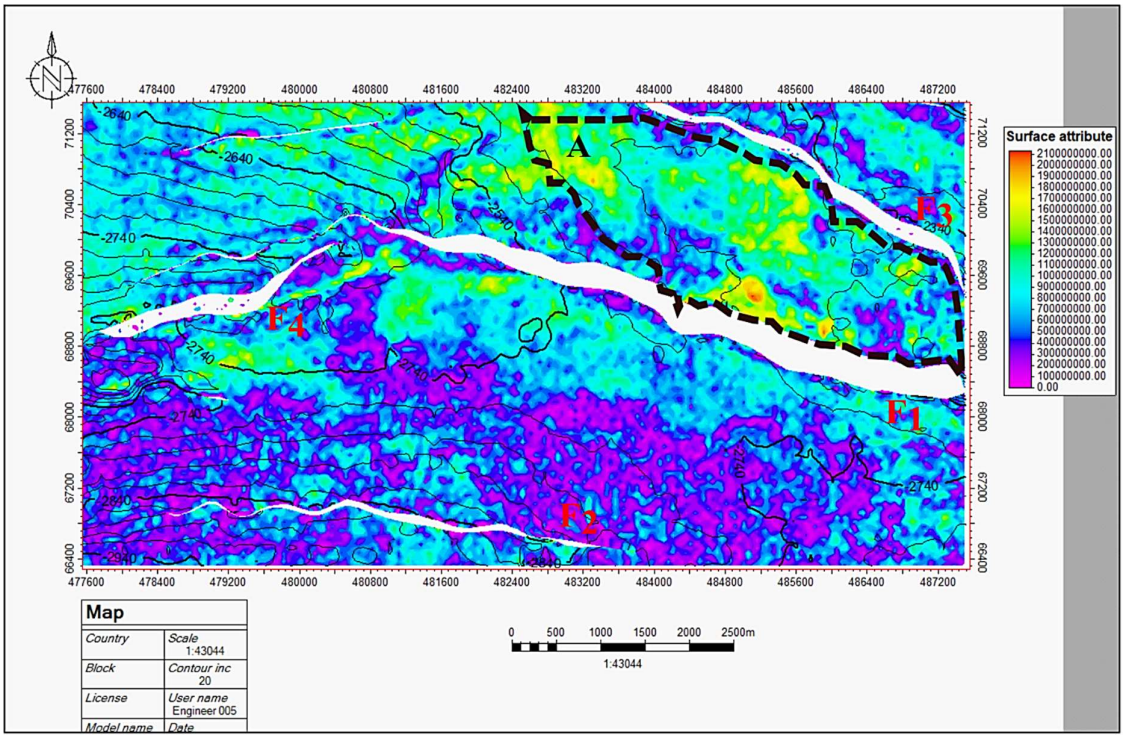


**Figure 21: Average Envelop attribute map for D-Surface of Jaff Field offshore Niger Delta.**

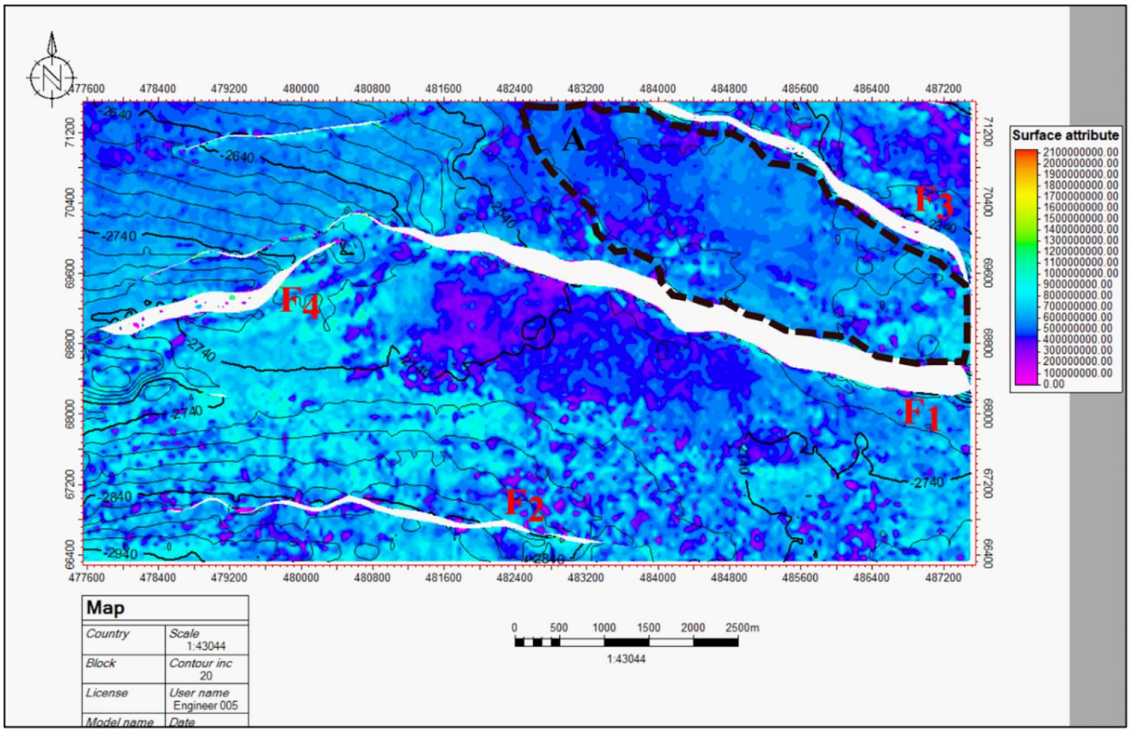


**Figure 22: Average Instantaneous Frequency attribute map for D-Surface of Jaff Field offshore Niger Delta.**

C**ONCLUSIONS**

The results from the 3D Seismic Attributes Analysis for Reservoir Characterization of Jaff Field Offshore Niger Delta, indicates that apart from the producing zone towards the western part of the field, that there is also an existence of other hydrocarbon prospective zones within the field. From well log data analysis, three hydrocarbon-bearing reservoirs were identified namely; Sand B, Sand C and Sand D. A well-to-seismic tie interpretation revealed that the tops of these hydrocarbon bearing reservoirs correspond nearly to the crests of the original seismic section which provide the two-way time and approx. depth.

Three horizons ($H_1$, $H_2$ and $H_3$) corresponding to near tops of delineated hydrocarbon-bearing sands were identified and studied after well -to- seismic tie. Eight faults were clearly mapped out. Moreover, maximum of four faults ($F_1$, $F_2$, $F_3$ and $F_4$) were shown on inline section 6180. These structures were mapped for the purpose of carrying out 3D subsurface structural interpretation, which were later used in generating the surface time-structural maps. These time-structural maps were subsequently converted to depth structural maps by applying the second-degree polynomial function. From the maps, it was observed that the principal structure responsible for hydrocarbon entrapment in the field for the three identified reservoirs are made up of a set of NW-SE trending normal faults. The lowest regions in the surface map are identified at the southern part, while the highest elevation is found at the northeastern region of the map.

Five prospects and one lead were identified in surface B. Prospect A has the largest zone (area), while prospect E has the smallest zone. Only one prospect was identified in surfaces C and D. These fault dependent traps (prospects) were further characterized by the presence of clusters of bright strong seismic attributes, (RMS, average envelop and average instantaneous frequency) showing potentially the presence of hydrocarbon in the regions.

# REFERENCES

Doust, N., & Omatsola, E. (1990). Niger Delta in Divergent passive margin basins, JD Edwards and PA Santogrossi, eds. *AAPG memoir*, *18*, 201-238.

Etu-Efeotor, J. O., (1997). Fundamen tals of Petroleum Geology. Paragraphics: *Port Harcourt,*

Evamy, B. D., Haremboure, J., Kamerling, P., Knaap, W. A., Molloy, F. A., & Rowlands, P. H. (1978). Hydrocarbon habitat of Tertiary Niger Delta: AAPG Bulletin, 62 (1), 1-39

Tuttle, M. L. W., Brownfield, M. E., & Charpentier, R. R., (1999). The Niger Delta Petroleum System. USGS Science for a changing world: *Open File Report* 65, 99-50.

Reijers, T. J. A., Petters, S.W. & Nwajide, C.S. (1997). The Niger Delta Basin*,* Africa Basins – Sedimentary Basin of the World 3: *Amsterdam, Elsevier Science*, 3, 151-172.

Short. K.C. & Stauble, A.J., 1967. Outline of geology of Niger Delta. *American Association of Petroleum Geologists Bull,* 51(5), 761-779.

Telford, W. M.; Geldart, L. P.; Sheriff, R. E. (1990). Applied Geophysicis. *Cambridge University Press*. 2nd Edition, 136 – 280.

Tuttle, M. L. W., Brownfield, M. E., & Charpentier, R. R., (1999). The Niger Delta Petroleum System. USGS Science for a changing world: *Open File Report* 65, 99-50.